Flow in thin films of superfluid ^{3}He on rough surfaces

1992 J. Phys.: Condens. Matter 4 9545

(http://iopscience.iop.org/0953-8984/4/48/010)

J. Phys.: Condens. Matter 4 (1992) 9545–9556. Printed in the UK

Flow in thin films of superfluid ^{3}He on rough surfaces

Lech S Borkowski†, Grzegorz Harań‡ and Lucjan Jacak‡

† Institut für Theorie der Kondensierten Materie, Universität Karlsruhe, D-7500 Karlsruhe 1, Federal Republic of Germany

‡ Institute of Physics, Wrocław University of Technology, Wyb. Wyspiańskiego 27, 50-370 Wrocław, Poland

Received 5 May 1992

Abstract. The superflow of ^{3}He in thin films on rough surfaces is studied using the formalism of microscopic theory. The gap equation is solved and the free energy and the superflow are calculated for three two-dimensional states that may exist in films with thickness $d \sim \xi_0$. In the absence of flow the two-dimensional B state and the two-dimensional A state are degenerate and energetically more favourable than other two-dimensional states. In the presence of flow the two-dimensional A state has the lowest energy. For increasing superflow there occurs a transition from the two-dimensional A state to the two-dimensional polar state. The order of this transition depends on temperature and the strength of pair breaking on the surface. The theory is compared with recent experimental results.

1. Introduction

Superfluid ^{3}He in restricted geometries is a subject of great interest. Experimental results point to non-trivial boundary effects for this system [1–6]. It is well known that ^{3}He, being a p-wave superfluid, is very sensitive to scattering off irregularities of the superfluid–solid interface [7]. The superfluid transition temperature is significantly reduced when at least one dimension of the system is of the order of the zero-temperature coherence length ξ_0. It turns out, however, that coating of the interface with up to several layers of ^{4}He changes the character of quasiparticle scattering from diffusive to specular [6]. In experiments [3, 4] the addition of ^{4}He brought the critical temperature of the film close to T_c for the bulk liquid. Since ^{4}He is preferentially adsorbed on the solid surface one is led to the conclusion that even small amounts of ^{4}He adsorbed on the surface (one or more layers) considerably reduces the pair breaking of the surface. One possible explanation for this effect is that the adsorbed atoms of ^{4}He smooth out irregularities of the surface. Nevertheless, it is clear that surface roughness on larger length scales remains almost unchanged since no more than a few layers of ^{4}He were present in the experiments in [3, 4]. This effect remains puzzling, although one might expect that spin relaxation at the boundary in pure ^{3}He contributes to the breaking of Cooper pairs, and consequently replacing solidified atoms of ^{3}He with ^{4}He cuts off the spin-scattering channel.

There have been efforts to study the problem near T_c using the Ginzburg–Landau formalism [8–13]. The obtained critical current [9] was found to follow a $(1 - T/T_c^F)^{3/2}$ dependence, T_c^F being the critical temperature of the film. However,

the most interesting experiments are currently being performed [2] beyond the GL regime. The quasiclassical method was also used to calculate the order parameter near surfaces [14], the critical current [15] and the density of states [16, 17]. The reader may consult any of these papers to find more references to the quasiclassical studies.

Here we use an alternative scheme, based on the Abrikosov–Gorkov method. Numerical calculations for the case of a thin film present no special difficulties, if one assumes a constant order parameter in the film. This should be a good approximation for two-dimensional phases. Our scheme can be used easily in any regular restricted geometry.

As described in [1], there are three length scales of the substrate roughness. We use a model of a rough surface that should be appropriate for small uncorrelated scattering centres. Since $\xi_0 \sim 60$ nm, this should be a good approximation for 'bumps' up to ~ 50 Å in diameter. The interaction of fermions with surface inhomogeneities is represented as 'white noise', changing the spectrum of single-particle excitations. This random process is called diffusive surface scattering.

In films with thickness $p_0^{-1} << d \sim \xi_0$, p_0 being the Fermi momentum of the bulk liquid, the likely candidates for the order parameter are the two-dimensional states considered by several authors [18, 19]. In the preceding paper [20] we have derived the gap equations, the free energy and the superflow for two-dimensional superfluid states in an arbitrary potential well. Here we apply this formalism to the case of a thin film on a rough substrate. In section 2 we present the model of this system and in section 3 we solve the gap equations and calculate the free energy for each of the states; section 4 contains results for the superflow and its comparison with available experimental data. We consider three states: two-dimensional polar, two-dimensional B and two-dimensional A states, all three being two-dimensional versions of their three-dimensional counterparts. We denote them by 2-P, 2-B and 2-A, respectively. They are introduced in [20]. The 2-A state, with $\Delta_1 \neq \Delta_2$, becomes more stable than the 2-B state when the symmetry in the plane of the film is broken by the superflow. The relative stability of the states 2-P and 2-A depends on temperature T, the superfluid velocity v and the pair-breaking strength Γ. Since we expect the interaction with the substrate to be the dominant factor determining the behaviour of the liquid in the thin film, we neglect the Fermi-liquid interaction between quasiparticles and treat the system as a Fermi gas. The pairing interaction is assumed [21] to be the same as in the bulk liquid. We assume $\hbar = k_B = 1$ throughout the calculation.

2. The model

We assume an infinite potential square well in the direction perpendicular to the surface. The substrate's roughness is represented by a Gaussian random height function $u(x, y)$ [21]:

$$\langle u(x, y)\rangle = 0 \tag{1}$$

$$\langle u(x, y)u(x', y')\rangle = w^2\delta(x - x')\delta(y - y'). \tag{2}$$

The parameter w describes the absolute magnitude of the surface irregularities. The interaction with the substrate in this model is a consequence of the boundary condition

for the single-particle wavefunction $\Psi(x, y, d + u(x, y)) = 0$, and $\Psi(x, y, 0) = 0$. For sufficiently small $u(x, y)$ this problem is essentially that of dirty superconductors and can be solved in an analogous way. The total number of Fermi circles below the chemical potential is ν_c, the nearest integer less than ν_0, where $\nu_0 = (2md^2\mu/\pi^2)^{1/2}$. More detailed descriptions of the model can be found in [21, 22]. For each of the Fermi circles we can now write the Abrikosov–Gorkov equations (the spin indices are suppressed here):

$$G_\nu(i\omega_n, p) = G_{0\nu}(i\omega_n, p) + G_{0\nu}(i\omega_n, p)\Delta_\nu(p)F_\nu^\dagger(i\omega_n, p) \tag{3}$$

$$F_\nu^\dagger(i\omega_n, p) = -G_{0\nu}^-(i\omega_n, p)\Delta_\nu^\dagger(p)G_\nu(i\omega_n, p). \tag{4}$$

The superscript '–' denotes time inversion. The Green function in the presence of surface scattering and superflow is

$$G_{0\nu}^{-1} = i\omega_n - \xi_p - \lambda_\nu - \Sigma_\nu(i\omega_n) - vp_F \tag{5}$$

where

$$\xi_p = \frac{p^2}{2m} - \mu \qquad \lambda_\nu = \frac{1}{2m}\left(\frac{\nu\pi}{d}\right)^2. \tag{6}$$

Here v is the superfluid velocity, λ_ν is the single-particle spectrum of states in the potential well, p is the momentum in the plane of the film and μ is the chemical potential of the system; p_F is given in [20]. The self-energy Σ_ν is due to the scattering at the surface and for each of the Fermi circles is given by [21, 22]

$$\Sigma_\nu(i\omega_n) = \frac{w^2}{2m^2d^2}\left(\frac{\nu\pi}{d}\right)^2\frac{1}{S}\sum_{p,\nu'}\left(\frac{\nu'\pi}{d}\right)^2 G_{\nu\prime}(i\omega_n, p) \tag{7}$$

where S is the surface area of the film. It is convenient to introduce a function $U(i\omega_n)$ and to write the self-energy in the following form:

$$\Sigma_\nu(i\omega_n) = -i\Gamma U(i\omega_n)\cos^2\theta_\nu \tag{8}$$

where Γ, being a function of w, is a measure of surface roughness:

$$\Gamma = \frac{\pi^4}{2md^2}\frac{w^2}{d^4}\nu_0^5. \tag{9}$$

The function $U(i\omega_n)$ turns out to be the solution of the following equation:

$$U(i\omega_n) = \sum_{\cos\theta_\nu}\cos^2\theta_\nu\int_{-\pi/2}^{\pi/2}\frac{d\phi}{\pi}|z_\nu|^{-1/2}\tilde{\omega}_n\sin\tfrac{1}{2}\phi(n,\nu) + \operatorname{sign}(\tilde{\omega}_n)vp_F\sin\theta_\nu\cos\phi\cos\tfrac{1}{2}\phi(n,\nu) \tag{10}$$

where

$$|z_\nu| = [(\tilde{\omega}_n^2 + \tfrac{3}{2}\Delta^2(\phi)\sin^2\theta_\nu - v^2p_F^2\sin^2\theta_\nu\cos^2\phi)^2 + 4v^2p_F^2\tilde{\omega}_n^2\sin^2\theta_\nu\cos^2\phi]^{1/2} \tag{11}$$

and

$$\cos\phi(n,\nu) = |z_\nu|^{-1}(-\tilde{\omega}_n^2 - \tfrac{3}{2}\Delta^2(\phi)\sin^2\theta_\nu + v^2 p_F^2 \sin^2\theta_\nu \cos^2\phi). \tag{12}$$

The terms $\cos\theta_\nu$ and $\sum_{\cos\theta_\nu}$ are defined as

$$\cos^2\theta_\nu = \left(\frac{\nu}{\nu_0}\right)^2 \qquad \sum_{\cos\theta_\nu} = \frac{1}{\nu_0}\sum_{\nu}$$

and

$$\tilde{\omega}_n = \omega_n + \Gamma U(i\omega_n)\cos^2\theta_\nu. \tag{13}$$

For each of the phases $\Delta^2(\phi)$ is given below.

3. The gap equations and the free energy

The order parameter can be written as [20]

$$\Delta_\nu(\hat{p}) = \sqrt{3/2}\sin\theta_\nu(\Delta_1\hat{p}_x + i\Delta_2\hat{p}_y)\sigma_z i\sigma_y \tag{14}$$

and

$$\Delta^2(\phi) = {\Delta_1}^2\cos^2\phi + {\Delta_2}^2\sin^2\phi \tag{15}$$

for the 2-A state, and

$$\Delta_\nu(\hat{p}) = \sqrt{3/2}\sin\theta_\nu[(\Delta_1\hat{p}_x - \Delta_2\hat{p}_y)\sigma_x + (\Delta_2\hat{p}_x + \Delta_1\hat{p}_y)\sigma_y]i\sigma_y \tag{16}$$

$$\Delta^2(\phi) = {\Delta_1}^2 + {\Delta_2}^2 = \Delta^2 \tag{17}$$

for the 2-B state. In the 2-P state $\Delta_1 = 0$ in equations (14) and (15); Δ_1 is chosen to be the gap in the direction of the flow. The gap equation for the 2-A state is the following:

$$\begin{Bmatrix}\Delta_1\\ \Delta_2\end{Bmatrix} = \begin{Bmatrix}\Delta_1\\ \Delta_2\end{Bmatrix} 6gN_0\frac{\pi^2}{p_0 d}T\sum_{\nu,\omega_n>0}\sin^2\theta_\nu\int_{-\pi/2}^{\pi/2}\frac{d\phi}{\pi}\begin{Bmatrix}\cos^2\phi\\ \sin^2\phi\end{Bmatrix}|z_\nu|^{-1/2}\sin\tfrac{1}{2}\phi(n,\nu). \tag{18}$$

In the equation above, g and N_0 are respectively the superfluid coupling constant and the density of states at the Fermi level, and p_0 is defined in [20]. For $\Delta_1 = 0$ the above equations apply to the 2-P state. The form of the gap equation used in numerical calculations is given in the appendix. Examples of solutions of the gap equations (18) and (22) at $T = 0.3T_{c0}$, T_{c0} being the critical temperature of the film with no pair breaking, are shown in figure 1. The terms Δ_1 and Δ_2 are double-valued functions of vp_F for lower temperatures. At $\Gamma = 0$ this double-valuedness is removed above $T \simeq 0.518T_{c0}$. The free energy can be found through the integration of equation (18) over self-energies Δ_1 and Δ_2 [20]. In a system with some form

of disorder the equation determining $U(i\omega_n)$, i.e. equation (10), must be integrated together with the gap equation (18). The free energy $F_S^A(\Delta_1, \Delta_2)$ of the superfluid system with disorder is then expressed as

$$F_S^A(\Delta_1, \Delta_2) - F_N = \int_0^{\Delta_1} f_1(\Delta_1', \Delta_2, U(i\omega_n))d\Delta_1' + \int_0^{\Delta_2} f_2(0, \Delta_2', U(i\omega_n))d\Delta_2'$$

$$+ \sum_n \int_{U_0}^{U(i\omega_n)} f_3(0, 0, U_n')dU_n'. \tag{19}$$

Here U_0 denotes $U(i\omega_n)$ in the normal phase:

$$U_0 \equiv U(i\omega_n)_{|\Delta_1=\Delta_2=0} = \frac{1}{\nu_0}\sum_\nu \cos^2\theta_\nu = \frac{\nu_c(\nu_c + 1/2)(\nu_c + 1)}{3\nu_0^3} \tag{20}$$

and the superscript 'A' stands for 2-A. F_N is the free energy of the normal phase. The functions f_1, f_2 and f_3 are given in the appendix. After performing some algebra we arrive, in equation (21), at the final result for the free energy:

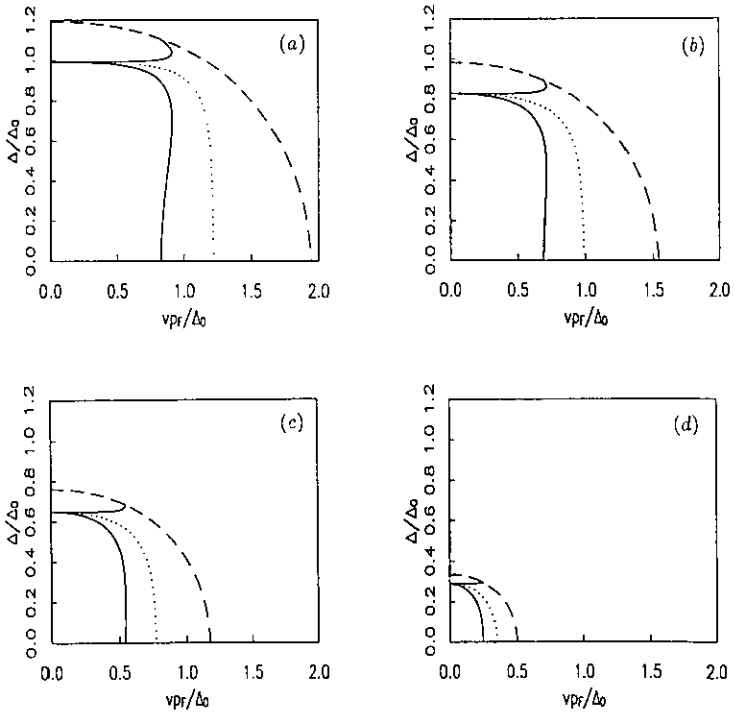

Figure 1. Solutions of the gap equation for the phases 2-A (full curve), 2-B (dotted curve) and 2-P (broken curve) at $T = 0.3T_{c0}$ for several values of the surface scattering strength Γ, (*a*) 0, (*b*) $0.1\Gamma_c$, (*c*) $0.2\Gamma_c$ and (*d*) $0.4\Gamma_c$. The term Γ_c is the critical scattering strength at $T = 0$ and $vp_F = 0$; Δ_0 is the gap at $T = 0$ and $vp_F = 0$.

$$F_S^A(\Delta_1,\Delta_2)-F_N = 3gN_0\frac{\pi^2}{p_0 d}T\Bigg(\sum_{\nu,\omega_n>0}\sin^2\theta_\nu\int_{-\pi/2}^{\pi/2}\frac{d\phi}{\pi}|z_\nu|^{-1/2}\Delta^2(\phi)\sin\tfrac{1}{2}\phi(n,\nu)$$

$$-\frac{4}{3}\sum_{\nu,\omega_n>0}\int_{-\pi/2}^{\pi/2}\frac{d\phi}{\pi}|z_\nu|^{1/2}\sin\tfrac{1}{2}\phi(n,\nu)$$

$$+\tfrac{4}{3}\nu_0\Gamma\sum_{\omega_n>0}\{U(i\omega_n)U_0+[U(i\omega_n)-U_0]^2\}\Bigg). \tag{21}$$

We can now analyze the relative stability of the different states. For small vp_F the 2-A state is always more stable than the 2-P state. However, for increasing vp_F there is a transition to the 2-P state. This transition is of first or second order, depending on temperature and the strength of surface scattering Γ, see figure 2. For smooth walls, $\Gamma = 0$, the transition is always of second order above $T \simeq 0.518T_{c0}$. For larger Γ, the interval of temperatures for which the first-order transition takes place is reduced. The 2-P-state to normal-state transition is always of second order.

The gap equation for the 2-B state is similar to equation (18):

$$\Delta = 3\Delta g N_0\frac{\pi^2}{p_0 d}T\sum_{\nu,\omega_n>0}\sin^2\theta_\nu\int_{-\pi/2}^{\pi/2}\frac{d\phi}{\pi}|z_\nu|^{-1/2}\sin\tfrac{1}{2}\phi(n,\nu). \tag{22}$$

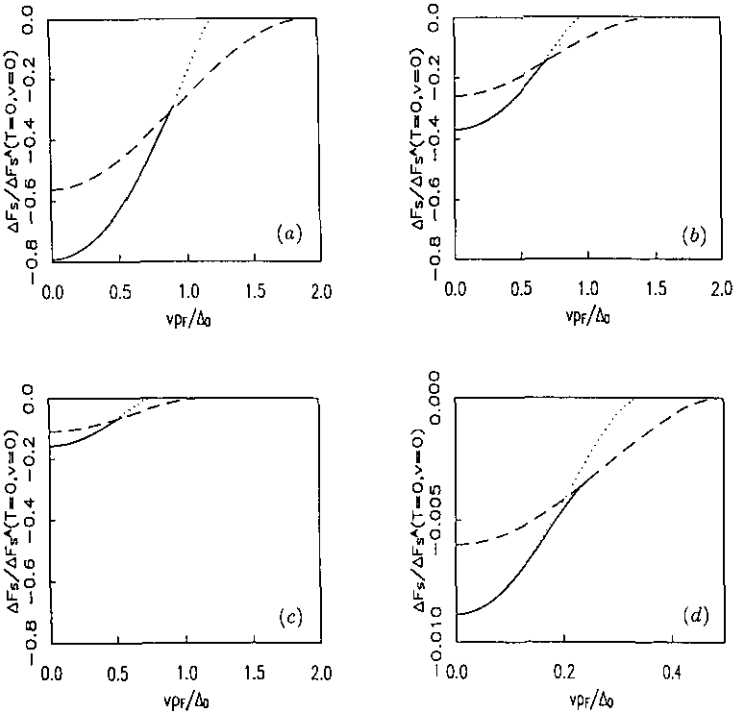

Figure 2. The free energy difference between the superfluid state and the normal state for all phases with the same parameter set as in figure 1. The curves are denoted as in figure 1. Here energy is scaled with respect to the energy difference between the 2-A phase and the normal state at zero temperature and no flow.

Here $\Delta = \sqrt{{\Delta_1}^2 + {\Delta_2}^2}$. The free energy of the 2-B state is found in the same way as in equation (21):

$$F_S^B(\Delta) - F_N = 3gN_0\frac{\pi^2}{p_0 d}T\Big(\sum_{\nu,\omega_n>0}\sin^2\theta_\nu\int_{-\pi/2}^{\pi/2}\frac{d\phi}{\pi}\Delta^2|z_\nu|^{-1/2}\sin\tfrac{1}{2}\phi(n,\nu)$$
$$-\frac{4}{3}\sum_{\nu,\omega_n>0}\int_{-\pi/2}^{\pi/2}\frac{d\phi}{\pi}|z_\nu|^{1/2}\sin\tfrac{1}{2}\phi(n,\nu)$$
$$+\tfrac{4}{3}\nu_0\Gamma\sum_{\omega_n>0}\{U(i\omega_n)U_0+[U(i\omega_n)-U_0]^2\}\Big). \tag{23}$$

The superscript 'B' refers to 2-B. For $v = 0$ the 2-A and 2-B states are degenerate, but for any $v > 0$ the 2-A state is more stable although the energy difference between these two states is always small. Figure 3 shows details of the phase diagram near the first-order transition from the 2-A to the 2-P state. In general, one cannot exclude the possibility that the relative stability of states in other theoretical calculations will change when additional features, which influence the self-energy, are introduced into the model.

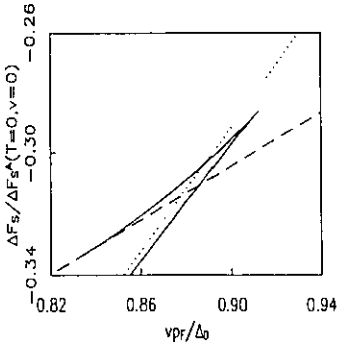

Figure 3. Details of the phase diagram near the first-order transition at $T = 0.3T_{c0}$ and $\Gamma = 0$.

4. The superflow

The superflow is given by

$$j_s = \frac{1}{V}T\sum_{\omega_n,\nu}\int\frac{d^2p}{(2\pi)^2}\frac{p+mv}{m}G_\nu(i\omega_n,p) \tag{24}$$

where V is the volume of the sample. Using the Green function derived in section 2, we arrive at

$$j_s = \frac{2(24\pi^5)^{1/6}}{(p_0 d\sum_\nu\sin^2\theta_\nu)^{1/2}}\rho^{2/3}T\sum_{\nu,\omega_n>0}\sin\theta_\nu\int_{-\pi/2}^{\pi/2}\frac{d\phi}{\pi}|z_\nu|^{-1/2}\cos\phi$$
$$\times\left(vp_F\sin\theta_\nu\cos\phi\sin\tfrac{1}{2}\phi(n,\nu)-\tilde{\omega}_n\cos\tfrac{1}{2}\phi(n,\nu)\right). \tag{25}$$

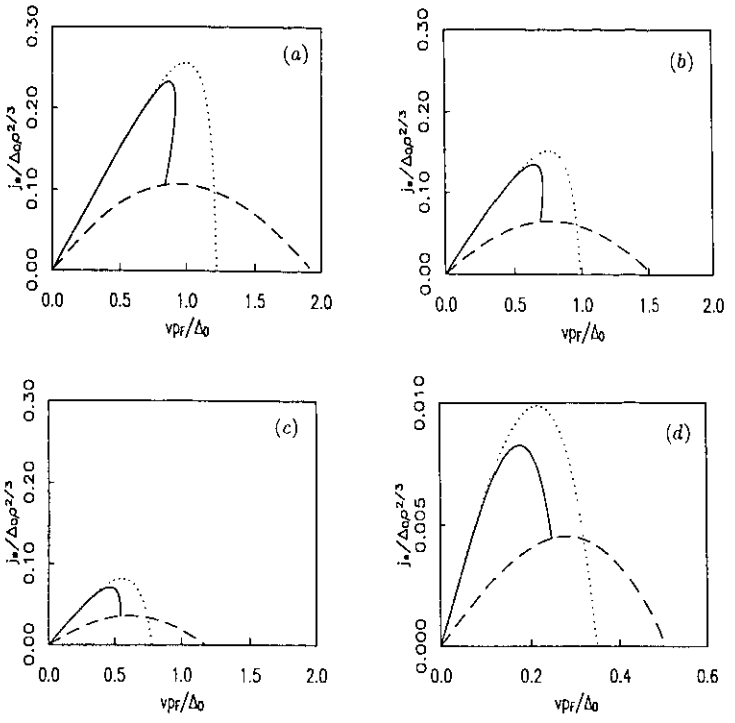

Figure 4. The superflow for the same parameter set as in figure 1 and with the same notation.

This equation holds for all three states. To find the maximum current j_{sc} with increasing vp_F one has to solve the gap equations and calculate the free energy. The maximum flow is always attained in the 2-A state. However, one must know the value of vp_F at the transition of the 2-A state into the 2-P state, since for a certain range of T and Γ the transition occurs *before* the current in the 2-A state would reach its absolute maximum. To illustrate this point, we plot in figure 4 the current for the same parameter set as in figures 1 and 2. Also, on comparing figures 2 and 4 we see that, although the largest flow might be achieved in the 2-B state, this state is not stable. Figure 5 shows the depression of the critical current density j_{sc} with increasing surface roughness. The dependence of j_{sc} on temperature is presented in figure 6. With the exception of very small temperatures, it follows the $(1-T/T_c^F)^{3/2}$ behaviour as is expected when the flow is limited by pair breaking. Comparing the magnitude of j_{sc} from our calculations to experimental results in figure 10 of [1] we find a significant difference. Although the phases seen in experiments may not be the same as the ones studied here, we think it is fair to compare at least orders of magnitude of critical currents for a given critical temperature in order to test the mechanism limiting critical currents in thin films. The experimental current density is several times smaller than that obtained from equation (25) for a given critical temperature of the film. This discrepancy also occurs [1] for j_{sc} in the GL theory of [9]. Another experimentally relevant quantity is the superfluid density ρ_s. From the critical temperature of the film we can find Γ and obtain ρ_s. However the experimental ρ_s is much smaller than in this pair breaking theory. Comparing our

result, figure 7, and figure 2 in [2], we see a significant difference. Finally, in figure 8 we show the dependence of the superfluid density on Γ.

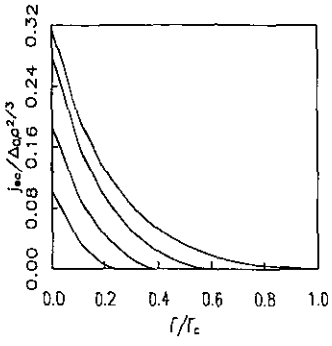

Figure 5. *Critical current density* j_{sc} as a function of increasing surface roughness at temperatures 0, $0.2T_{c0}$, $0.4T_{c0}$ and $0.6T_{c0}$.

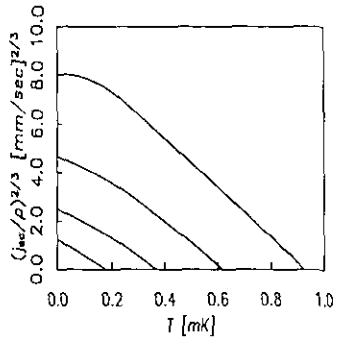

Figure 6. Critical current density j_{sc} as a function of temperature for several values of pair-breaking strength at the surface: 0, $0.2\Gamma_c$, $0.4\Gamma_c$ and $0.6\Gamma_c$. The film thickness was chosen to be in the range measured in [1].

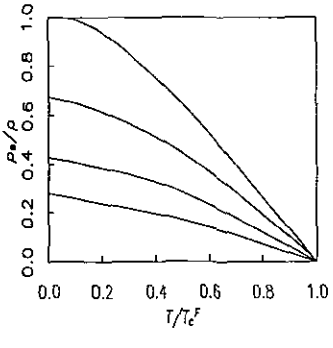

Figure 7. Superfluid density against temperature. The temperature is scaled to the critical temperature in the film. The values of Γ are the same as in figure 6.

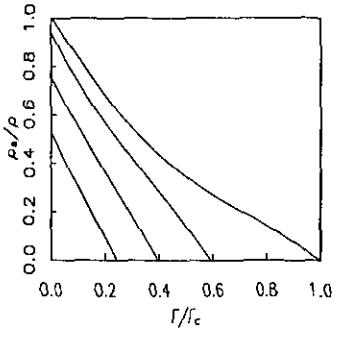

Figure 8. Superfluid density as a function of Γ at four temperatures: 0, $0.2T_{c0}$, $0.4T_{c0}$ and $0.6T_{c0}$.

5. Conclusion

We have studied the properties of two-dimensional states of superfluid ^{3}He in films on rough surfaces including the effects of superflow.

We found that the 2-A and 2-P states are always more stable than the 2-B state for non-zero superflow. Apart from reducing the critical temperature of the film and the superflow, both facts already well known, surface roughness has an important effect

on the order of the phase transition between the 2-A and the 2-P state. Increasing strength of pair breaking at the surface moves the critical point between the first- and second-order transition line to lower temperatures. However, the critical point is not removed from the phase diagram. With increasing Γ it approaches $T = 0$, but does not disappear from the phase diagram until superfluidity is destroyed entirely.

It becomes apparent that pair breaking alone does not suffice to explain the flow experiments in superfluid ^{3}He films. The next logical step towards a satisfying theory of this system is the inclusion of more realistic boundary conditions for the superfluid–normal interface in restricted geometry, perhaps along the lines suggested recently by two groups of authors [23, 24]. The creation of vortices may also substantially reduce critical currents [25]. We have not considered large surface irregularities, which may have a significant effect on j_{sc}. The liquid over large bumps on the surface may be thinner and those areas may substantially reduce the critical current. A related question is the proper description of scattering processes at the superfluid–solid interface. The addition of a small amount of ^{4}He, the equivalent of only about two layers, to superfluid ^{3}He films [3, 4] was enough to increase T_c to almost its bulk value. Since the roughness of the liquid–solid boundary was not removed, except perhaps for bumps on the atomic scale, it may seem that the effect of the surface in the absence of superflow is mostly to break pairs through spin relaxation at the walls. So far the spin-flip scattering at interfaces of ^{3}He is not well characterized and the spin-relaxation times at the boundaries of experimental cells are largely unknown. This fact was particularly emphasized by Meyerovich [26] in the context of studies of spin-polarized normal ^{3}He. However, in a recent experimental study of the effect of ^{4}He at surfaces with roughness on the scale of 20 Å in normal ^{3}He [27] the authors suggest that increased specularity of surfaces coated by ^{4}He is not due to the replacement of the localized magnetic layer of ^{3}He. It is likely that momentum transfer from the surface to the superfluid ^{3}He is reduced by the presence of the ^{4}He film [27, 28], perhaps due to the superfluidity of the ^{4}He film [27].

We can thus conclude that the interpretation of experiments on superflow in thin films of ^{3}He is hindered by insufficient knowledge of processes occurring at the superfluid–solid interface.

Acknowledgment

We would like to thank Professor M Salomaa for helpful comments.

Appendix.

To solve the gap equation numerically, we transform it into

$$\ln\left(\frac{T}{T_{c0}}\right) = 7.12\alpha\frac{T}{T_{c0}}\frac{1}{\sum_\nu \sin^2\theta_\nu}\sum_{\nu,n\geqslant 0}\sin^2\theta_\nu \int_{-\pi/2}^{\pi/2}\frac{d\phi}{\pi}\begin{Bmatrix}\cos^2\phi\\ \sin^2\phi\end{Bmatrix}|z_\nu|^{-1/2}\sin\tfrac{1}{2}\phi(n,\nu) - \sum_{n\geqslant 0}\frac{1}{n+1/2} \tag{A1}$$

where the temperature and the order parameter are now scaled with respect to their magnitudes in a film with no pair breaking, T_{c0} and Δ_0, respectively. The term Δ_0 is the gap at $T = 0$ and $v = 0$. Equations (10)–(12) are then rewritten with the following changes:

$$\tilde{\omega}_n \to 1.78\alpha(2n+1)\frac{T}{T_{c0}} + \frac{\Gamma}{\Delta_0}U(i\omega_n)\cos^2\theta_\nu \tag{A2}$$

$$\Delta^2(\phi) \to \Delta^2(\phi)/\Delta_0 \qquad v p_F \to v p_F/\Delta_0 \tag{A3}$$

where

$$\alpha = \exp(\langle \ln\sin\theta_\nu\rangle) \qquad \langle \ln\sin\theta_\nu\rangle \equiv \left(\sum_\nu \sin^2\theta_\nu\right)^{-1}\sum_\nu \sin^2\theta_\nu \ln\sin\theta_\nu. \tag{A4}$$

The integrands f_1 and f_2 in equation (19) are

$$\begin{Bmatrix} f_1(\Delta_1,\Delta_2,U(i\omega_n)) \\ f_2(\Delta_1,\Delta_2,U(i\omega_n)) \end{Bmatrix} \equiv \begin{Bmatrix} \Delta_1 \\ \Delta_2 \end{Bmatrix} - 6gN_0\frac{\pi^2}{p_0 d}T\sum_{\nu,\omega_n>0}\sin^2\theta_\nu\int_{-\pi/2}^{\pi/2}\frac{d\phi}{\pi}\begin{Bmatrix} \Delta_1\cos^2\phi \\ \Delta_2\sin^2\phi \end{Bmatrix}$$
$$\times \mathrm{Re}\{[(\tilde{\omega}_n + iv p_F\sin\theta_\nu\cos\phi)^2 + \tfrac{3}{2}\Delta^2(\phi)\sin^2\theta_\nu]^{-1/2}\}. \tag{A5}$$

At $f_1 = 0$ and $f_2 = 0$ these two equations are just the gap equations, written in a form more convenient for integration. The term f_3 is given by

$$f_3(\Delta_1,\Delta_2,U(i\omega_n)) \equiv 6gN_0T\nu_0\Gamma\frac{\pi^2}{p_0 d}\left[U(i\omega_n) - \sum_{\cos\theta_\nu}\cos\theta_\nu\int_{-\pi/2}^{\pi/2}\frac{d\phi}{\pi}\right.$$
$$\left.\times\,\mathrm{Re}\left(\frac{\tilde{\omega}_n + iv p_F\sin\theta_\nu\cos\phi}{[(\tilde{\omega}_n + iv p_F\sin\theta_\nu\cos\phi)^2 + \tfrac{3}{2}\Delta^2(\phi)\sin^2\theta_\nu]^{1/2}}\right)\right]. \tag{A6}$$

The numerical calculations of j_s given by equation (25) are carried out using equations (A2)–(A4).

References

[1] Daunt J G, Harris-Lowe R F, Harrison J P, Sachrajda A, Steel S C, Turkington R R and Zawadzki P 1988 *J. Low Temp. Phys.* **70** 547

[2] Xu J and Crooker B C 1990 *Phys. Rev. Lett.* **65** 3005

[3] Harrison J P, Sachrajda A, Steel S C and Zawadzki P 1991 *Excitations in Two-Dimensional and Three-Dimensional Quantum Fluids* ed A G F Wyatt and H J Lauter (New York: Plenum)

[4] Steel S C, Zawadzki P, Harrison J P and Sachrajda A 1990 *Physica* B **165/166** 599

[5] Davis J C, Amar A, Pekola J P and Packard R E 1988 *Phys. Rev. Lett.* **60** 302

[6] Freeman M R and Richardson R C 1990 *Phys. Rev.* B **41** 11011 and references therein

[7] Ambegaokar V, de Gennes P G and Rainer D 1974 *Phys. Rev.* A **6** 2676

[8] Barton G and Moore M A 1975 *J. Low Temp. Phys.* **21** 489

[9] Jacobsen K W and Smith H 1987 *J. Low Temp. Phys.* **67** 83

[10] Kjäldman L H, Kurkijärvi J and Rainer D 1978 *J. Low Temp. Phys.* **33** 577

[11] Fetter A L and Ullah S 1988 *J. Low Temp. Phys.* **70** 515

[12] Adamenko I N and Poluéktov Yu M 1985 *Fiz. Nizk. Temp.* **11** 353 (Engl. transl. 1985 *Sov. J. Low Temp. Phys.* **11** 191)
[13] Li Y H and Ho T-L 1988 *Phys. Rev.* B **38** 2362
[14] Zhang W, Kurkijärvi J and Thuneberg E V 1987 *Phys. Rev.* **36** 1987
[15] Ullah S and Buchholtz L J 1989 *Phys. Rev.* B **40** 8791
[16] Buchholtz L J 1991 *Phys. Rev.* B **44** 4610
[17] Kopnin N B, Soininen P I and Salomaa M M 1991 *J. Low Temp. Phys.* **85** 267
[18] Brusov P N and Popov V N 1982 *Phys. Lett.* **87A** 472
[19] Stein D L and Cross M C 1979 *Phys. Rev. Lett.* **42** 504
[20] Harań G and Jacak L 1992 *J. Phys.: Condens. Matter* **4** 9531–44
[21] Tešanović Z and Valls O T 1986 *Phys. Rev.* B **34** 7610
[22] Harań G, Jacak L and Borkowski L S 1989 *Physica* B **159** 223
[23] Grabinski M and Liu M 1988 *J. Low Temp. Phys.* **73** 79
[24] Sun Y, Wölfle P, Yip S K and Cross M C 1990 *J. Low Temp. Phys.* **80** 237
[25] Kopnin N B, Soininen P I and Salomaa M M 1992 *Phys. Rev.* B **45** 5491
[26] Meyerovich A E 1990 *Helium Three* ed W P Halperin and L P Pitaevskii (Amsterdam: North-Holland)
[27] Tholen S M and Parpia J M 1991 *Phys. Rev. Lett.* **67** 334
[28] Ritchie D A, Saunders J and Brewer D F 1987 *Phys. Rev. Lett.* **59** 465